MAYO CLINIC

MAYO CLINIC PROCEEDINGS: DIGITAL HEALTH

ORIGINAL ARTICLE

Hemorrhage Evaluation and Detector System for Underserved Populations: HEADS-UP

Saif Salman, MD; Qiangqiang Gu, PhD; Benoit Dherin, PhD; Sanjana Reddy, MS; Patrick Vanderboom, PhD; Rohan Sharma, MBBS; Lin Lancaster, PhD; Rabih Tawk, MD; and William David Freeman, MD

Abstract

Objective: To create a rapid, cloud-based, and deployable machine learning (ML) method named hemorrhage evaluation and detector system for underserved populations, potentially across the Mayo Clinic enterprise, then expand to involve underserved areas and detect the 5 subtypes of intracranial hemorrhage (IH).

Methods: We used Radiological Society of North America dataset for IH detection. We made 4 total iterations using Google Cloud Vertex AutoML. We trained an AutoML model with 2000 images, followed by 6000 images from both IH positive and negative classes. Pixel values were measured by the Hounsfield units, presenting a width of 80 Hounsfield and a level of 40 Hounsfield as the bone window. This was followed by a more detailed image preprocessing approach by combining the pixel values from each of the brain, subdural, and soft tissue window-based gray-scale images into R(red)-channel, G(green)-channel, and B(blue)-channel images to boost the binary IH classification performance. Four experiments with AutoML were applied to study the effects of training sample size and image preprocessing on model performance.

Results: Out of the 4 AutoML experiments, the best-performing model was the fourth experiment, where 95.80% average precision, 91.40% precision, and 91.40% recall were achieved. On the basis of this analysis, our binary IH classifier hemorrhage evaluation and detector system for underserved populations appeared both accurate and performed well.

Conclusion: Hemorrhage evaluation and detector system for underserved populations is a rapid, cloud-based, deployable ML method to detect IH. This tool can help expedite the care of patients with IH in resource-limited hospitals.

 ■ Mayo Clin Proc Digital Health 2023;1(4):547-556

Strokes are the second most common cause of death and disability globally.[1] Although ischemic strokes are more prevalent (80%-85%), hemorrhagic strokes are considered deadlier and more disabling. On the basis of anatomical distribution, intracranial hemorrhagic (IH) includes 5 subtypes: intracerebral hemorrhage (ICH), subarachnoid hemorrhage, subdural hematoma, epidural hematoma, and intraventricular hemorrhage. The subdural and epidural subtypes are commonly associated with traumatic brain injuries, whereas the intraparenchymal, subarachnoid, and intraventricular subtypes result from bleeding tumors, vascular malformations, and vasculitis.[2,3]

Intracerebral hemorrhage is the most common subtype of IH, carrying an average mortality rate of 40% by 30 days[4] and can reach up to 60% in one year.[5] Low Glasgow coma scale, hemorrhage volume exceeding 30 mL, extension into ventricles, infratentorial hemorrhage, or subsequent hemorrhage in deep structures such as the basal ganglia, pons, or cerebellum are associated with a poor outcome.[2,6] Other risk factors for increased ICH mortality are increasing age, woman sex, rurality, and history of long-term illnesses.[7]

From the Departments of Neurological Surgery, Neurology and Critical Care, Mayo Clinic, Jacksonville, FL (S.S., R.S., R.T., W.D.F.); Health Sciences Research, Mayo Clinic Graduate School of Biomedical Sciences (Q.G.) and Department of Laboratory Medicine and Pathology (P.V.), Mayo Clinic, Rochester, MN; Google, Inc, Mountain View, CA (B.D., S.R.); and Center for Digital Health, Mayo Clinic, Phoenix, AZ (L.L.).

Despite the etiologies, the use of anticoagulants, particularly if combined with the aforementioned factors, potentiates the risk of expansion and rebleeding with a 0.6% risk or less per year.[8]

Primary ICH can be caused by hypertension, atherosclerosis, or amyloid angiopathies. To a lesser extent, ruptured aneurysms, bleeding tumors, vascular malformations, coagulopathies, and previous thrombolysis can cause secondary ICH.[2] Patients develop a myriad of short-term and long-term complications ranging from rebleeding, expansion, vasospasm, seizures, cognitive decline, and multisystemic neurological injuries inflicted on the myocardium and lungs.[2]

Early detection and timely intervention is paramount and crucial in determining outcome.[3] Regrettably, although medical history can be the first guide toward unraveling the etiology of strokes,[9] sole clinical examination lacks a particular role in distinguishing ischemic from hemorrhagic strokes as the presenting symptoms can be somewhat similar. Hence, noncontrast head computed tomography scans (NCCT) remain the gold standard differentiation method.[2,10-13] However, despite studies reporting high sensitivity and specificity for NCCT scans in ICH detection,[14-16] using automated IH detection models is crucial to achieving high accuracy, reliability, and speed. Delays in detection with subsequent delays in management, particularly in the first hour, will result in hemorrhage expansion and worse outcomes. Unlike ischemic strokes, where thrombectomies can preserve neuronal viability, IH in general and ICH in particular lack such management options, particularly when detection is delayed.[2,17,18]

Machine learning (ML) uses unique models such as feedforward artificial neural networks, random forest, support vector machine, logistic regression, stacked convolutional denoizing auto-encoders, principal component analysis, and multilayer perceptron. The aforesaid feedforward artificial neural networks are the most used to predict case-specific outcomes, competing with the decisions made by clinicians.[19-21]

Since 2018, there has been a paradigm shift in the management of ischemic strokes through the implementation of artificial intelligence (AI) and ML methods in processing NCCT and CT perfusion scans to predict large vessel occlusion in the prehospital setting, improve precise detection of clots, decrease latency until intervention, improve reperfusion, and predict clinical outcomes.[22-27]

Patients with IH lack such a predictive model in a streamlined system to improve acute stroke systems of care, earlier detection, and outcome. There is an unfulfilled need to create an earlier IH detection method that accelerates interventions. Hemorrhage evaluation and detector system for underserved populations (HEADS-UP) is a high-precision, rapid, and cloud-based deployable model created using Google Cloud VertexAI AutoML to detect IH remotely. Hence, HEADS-UP can detect IH in a time-efficient manner, make the most of our health system, and improve outcomes. We aim to implement HEADS-UP across the Mayo Clinic enterprise and expand to include underserved areas.

The main novelty in HEADS-UP is on the basis of the incorporated joint efforts between ML scientists, neurologists, and neurosurgeons to generate a deployable and high-precision model within 2 weeks and individualize it toward patient care, future discovery, and translation of sciences.

METHODS

Dataset

We aim to develop a binary image classifier to identify positive IH cases in 2-dimensional NCCT images. We downloaded the original dataset from the Radiological Society of North America (RSNA) IH database. The RSNA dataset is a noncommercial, open-label, and free dataset that includes 874,035 scans from different institutions worldwide. It is dedicated for ML purposes. A large number of neuroradiologists volunteered to iterate and classify IH subtypes.[28] The images in the dataset were categorized into 7 annotation groups representing the 5 known IH subtypes (intraparenchymal, subarachnoid, subdural, intraventricular, and epidural), along with another group that includes nonhemorrhage.[28] Totally, we attained 752,803 labeled images (Table 1).

Data Preprocessing

After excluding duplicates, we pooled the images from the 6 IH subtypes as a single IH

Mayo Clin Proc Digital Health ■ December 2023;1(4):547-556 ■ https://doi.org/10.1016/j.mcpdig.2023.08.009
www.mcpdigitalhealth.org

TABLE 1. Summary of Radiological Society of North America (RSNA) Intracranial Hemorrhage(IH) Dataset Information

RSNA IH Dataset Category	Number of Images	Reassigned Labels for HEADS-UP
Intracerebral or intraparenchymal	36,118	Hemorrhage positive
Subarachnoid	35,675	Hemorrhage positive
Subdural	47,166	Hemorrhage positive
Intraventricular	26,205	Hemorrhage positive
Epidural	3145	Hemorrhage positive
Nonhemorrhage	644,870	Hemorrhage negative

HEADS-UP, hemorrhage evaluation and detector system for underserved populations.

positive class and images from the nonhemorrhage group as the IH negative class to apply a binary image classifier and detect IH cases when present. Two thousand randomly selected images were used for model development and testing, including 1000 images from each IH positive and negative class. To better understand the effect of training sample size on model performance, we created another dataset using the same method but with 6000 images, including 3000 images from each IH positive and negative class.

Original image data from the RSNA hemorrhage dataset was saved in digital imaging and communications in medicine standard format.[29] Because the VertexAI AutoML did not directly support the digital imaging and communications in medicine format, the raw image pixel arrays were extracted from the digital imaging and communications in medicine files and were saved as Portable Network Graphic formats.

We further arranged each image into brain, subdural, and soft tissue windows with different Hounsfield units. The difference in the Hounsfield units enhanced further differentiation between IH and non-IH cases. An additional approach combined the pixel values from each of the brain, subdural, and soft tissue window gray-scale images into 3-channeled R(red), G(green), and B(blue) (RGB) images.

To be more precise, each of the original Portable Network Graphic format pixel arrays was filtered into brain, subdural, and soft tissue windows on the basis of their unique window width and level values in Hounsfield units. The brain window has a width value of 80 Hounsfield units and a level value of 40 Hounsfield units. The subdural window has a width value between 130 and 300 Hounsfield units and a level value between 50 and 100 Hounsfield units. The soft tissue window has a width value of 250 to 400 Hounsfield units and a level value of 50 Hounsfield units.[30,31] Then, the 512 × 512-dimensional pixel arrays of the brain, subdural, and soft tissue window gray-scale images were placed into the red, green, and blue channels to form the RGB images.

The final combined 3-channeled RGB images were used to train AutoML-based binary IH classifiers and to design an inclusive hemorrhage detector for the 5 IH subtypes. The images with the corresponding labels were randomly split into 90% for model development and 10% for model testing and applied to each patient level.

Model Training and Testing

Images within the model development sets were used to optimize model predictions during the training phase. However, images in the testing set were used to evaluate the performance of the developed model.

We applied the eXplanation with Ranked Area Integrals (XRAI) method, the latest approach for AI model interpretation. XRAI uses region-based image attribution to determine regions from the inference images with the highest predictions for binary IH classes.[32] Furthermore, XRAI combines the integrated gradients method with additional steps to determine regions with the highest contributions for class prediction. The implementation of this study was programmed in Python (Python 3.11), and the data preprocessing source

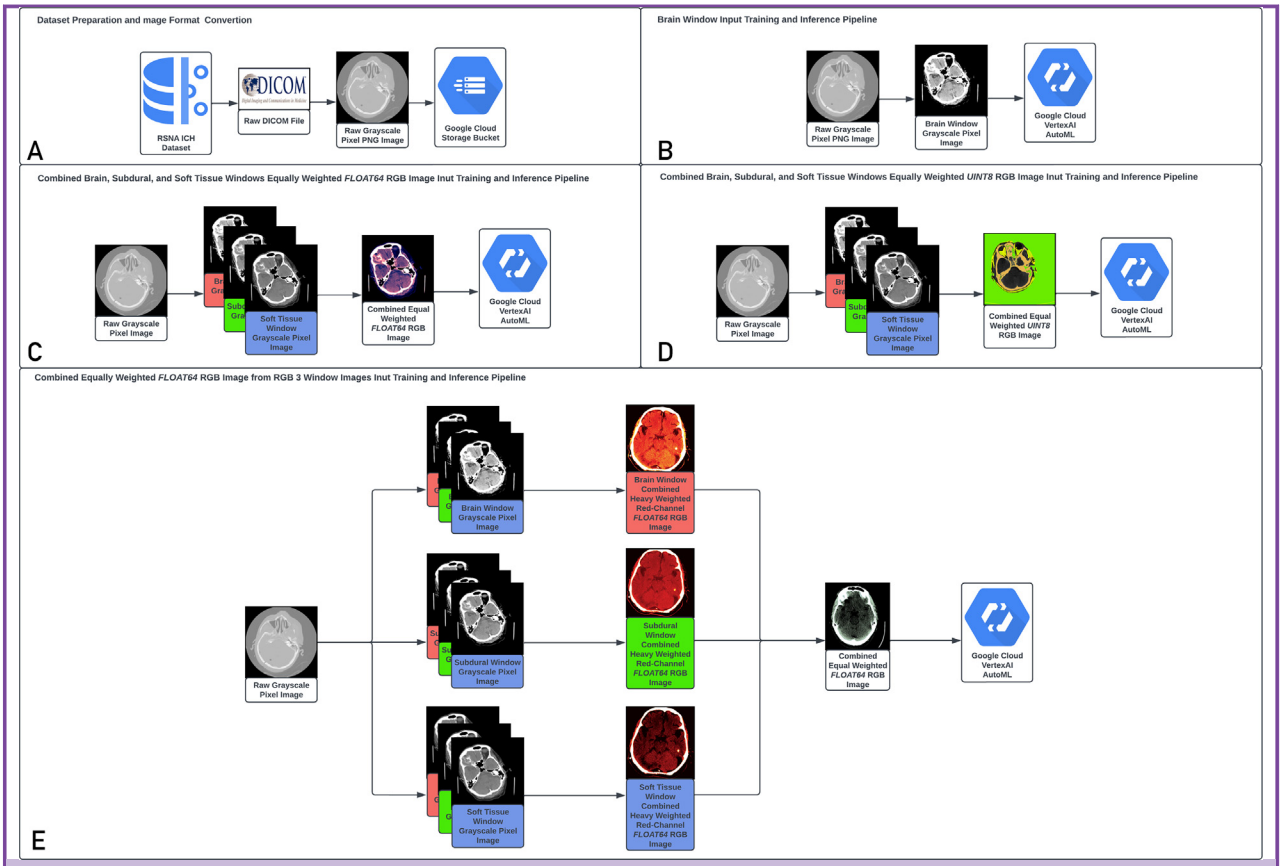

FIGURE 1. Diagram of the entire dataset preparation, image preprocessing, model training, and inference pipeline. (A) Dataset preparation including downloading original DICOM format files from the RSNA dataset and converting DICOM format image into PNG format. (B) Image preprocessing for AutoML training and inference pipeline, which corresponds to the experiment indexed as E1 in Supplementary Table 1, available online at https://www.mcpdigitalhealth.org/. (C) Image preprocessing for AutoML training and inference pipeline, which corresponds to the experiment indexed as E2 in Supplementary Table 1. (D) Image preprocessing for AutoML training and inference pipeline, which corresponds to the experiment indexed as E3 in Supplementary Table 1. (E) Image preprocessing for AutoML training and inference pipeline, which corresponds to the experiment indexed as E4 in Supplementary Table 1. DICOM, digital imaging and communications in medicine; RSNA, Radiological Society of North America.

code is publicly available at https://github.com/quincy-125/MG-HEADSUP.

Four experiments were executed to fully understand the effects of training sample size and data preprocessing on AutoML-based binary IH classification performance (Supplementary Table 1, available online at https://www.mcpdigitalhealth.org/). We started by increasing the training sample size from 2000 to 6000. We further trained the binary IH classifier on gray-scale images with pixel values filtered by the Hounsfield unit range corresponding to the brain window. This was followed by training the binary IH classifier on the combined 3-channel RGB images.

The first experiment was training the AutoML model on 2000 gray-scale brain window images (E1). The following 3 experiments used the combined 3-channeled RGB images to train the binary IH classifier. The second experiment (E2) assigned equal weight to every pixel from the red, green, and blue channels. The resulting pixel values from the combined 3-channeled RGB images were saved as floating numbers with 64 bits (float64). The third experiment (E3) is similar, but the resulting pixel values from the combined 3-

TABLE 2. Inference Results for Each of the 4 Experiments

Experiment Index	Recall (Threshold=0.5)	Precision (Threshold=0.5)	Average Precision
E1	88.90%	88.90%	91.50%
E2	90.00%	90.00%	95.20%
E3	90.00%	90.00%	95.20%
E4	91.40%	91.40%	95.80%

channeled RGB image were saved in the format of integers with 8 bits (uint8).

The last experiment (E4) was performed best by duplicating the pixels from each brain, subdural, and soft tissue window gray-scale image to generate window-based combined RGB images with heavily-weighted red channel pixel values. We further combined each of the 3 window-based RGB images and produced the final combined equally-weighted RGB image with each pixel value saved in the float64 format (Figure 1).

RESULTS

Precision and recall values were reported for each of the 4 experiments discussed in the model training and testing section with a threshold value of 0.5. In addition, average precision (the area under the precision-recall curve) was considered as a measurement of our models' performance. All of the reported statistical metrics regarding each of the 4 experiments are listed in Table 2.

The precision-recall curve, including the precision and recall values along different thresholds, is reported for all 4 experiments (Figure 2). Out of the 4 experiments conducted through our AutoML model, the experiment E4 achieved the highest performance in terms of average precision (95.80%) relative to the other experiments (E1: 91.50%, E2: 95.20%, and E3: 95.20%). For example, at an equal error rate cutoff, E4 achieves a precision-recall of (91.40% and 91.40%), E1 a precision-recall of (88.90% and 88.90%), E2 a precision-recall of (90.00% and 90.00%), and E3 a precision-recall of (90.00% and 90.00%).

DISCUSSION

Intracranial hemorrhage causes the highest stroke mortality rates in rural areas and underserved populations. This can be attributed to limited health education, primary prevention, and access to health care. However, the need for early detection owing to the absence of transportation methods, imaging facilities, or health care professionals capable of interpreting the imaging results is still the most profound factor affecting management and outcome.[33-37] Although modifiable risk factors remain a focus of interest, providing a streamlined approach to expedite IH diagnosis followed by guided management in the acute phase is critical to improving outcomes.

Given the rising era of AI and ML in various medical fields and the application of ML in diagnosing ischemic strokes and predicting large vessel occlusion, we perceive similar roles in processing NCCT scans and diagnosing IH. These roles improved accuracy, time latency, and outcome. Davis et al[38] incorporated an ML algorithm, "Aidoc," on the basis of a convolutional neural network to detect ICH on the NCCT scans. They reported reduced turnaround time to detect hemorrhage during the acute phase, but no change in the length of emergency department stay compared with patients with non-ICH.[38] Arbabshirani et al[39] aimed to develop a model capable of detecting ICH through large numbers of head NCCT scans and predict the reduction in time taken for interpretation. They reported decreased latency for interpretation by 96% and the ability to identify missed hemorrhages by radiologists. Furthermore, Lyu et al[40] used logistic regression analysis of NCCT scans for 238 patients to report a diagnostic accuracy that surpasses that of radiologists when differentiating between primary and secondary ICH. They also reported that lobar hemorrhages in women could be correlated with secondary ICH, whereas hypertension will most likely cause primary ICH in all patients.[40]

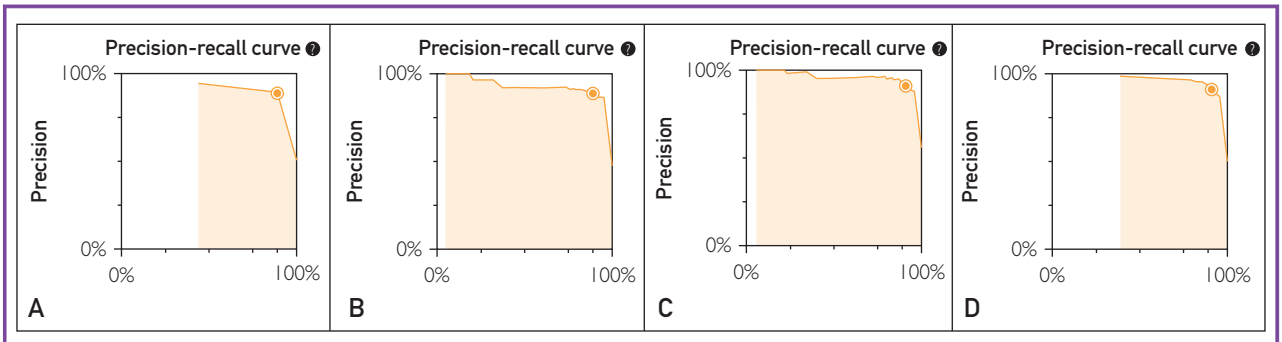

FIGURE 2. Precision-Recall Curve for experiments E1 to E4. (A) Precision-Recall Curve for E1. (B) Precision-Recall Curve for E2. (C) Precision-Recall Curve for E3. (D) Precision-Recall Curve for E4.

We created HEADS-UP using Google Cloud VertexAI AutoML, which automatically identifies the most appropriate models to maximize the binary IH classification performance and design an inclusive IH detector. Hemorrhage evaluation and detector system for underserved populations is a cloud-based, rapid, and deployable algorithm to detect IH primarily in smaller hospitals in underserved areas, which could help put earlier attention on these

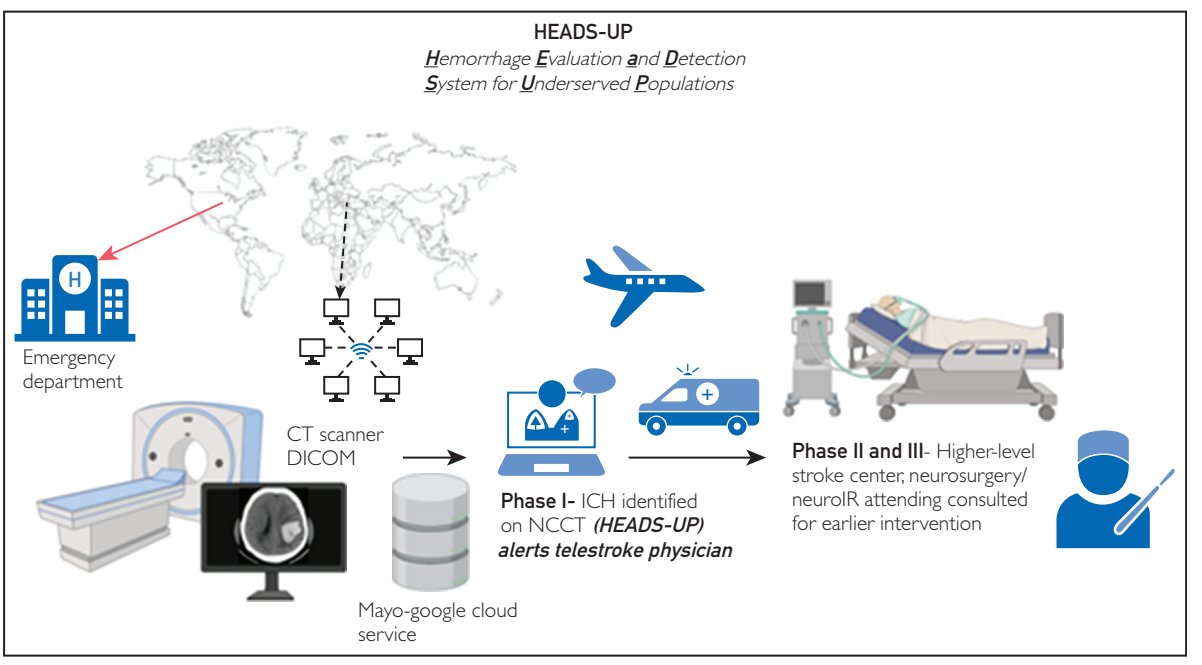

FIGURE 3. Courtesy of co-author WDF, describes the role of HEADS-UP to detect IH in the underserved areas and expedite efficient and timely intervention. Starting from Mayo Clinic followed by deployment in underserved areas with limited health care resources, HEADS-UP can expedite detection of IH (phase I) which alerts stroke physicians to coordinate with other attendings in the Neurological Surgery and the Interventional Neuroradiology departments (phases II and III) to ensure expedited patient transfer and planned intervention in a coordinated effort and timely fashion. HEADS-UP, hemorrhage evaluation and detector system for underserved populations; IH, intracranial hemorrhage.

Mayo Clin Proc Digital Health ■ December 2023;1(4):547-556 ■ https://doi.org/10.1016/j.mcpdig.2023.08.009
www.mcpdigitalhealth.org

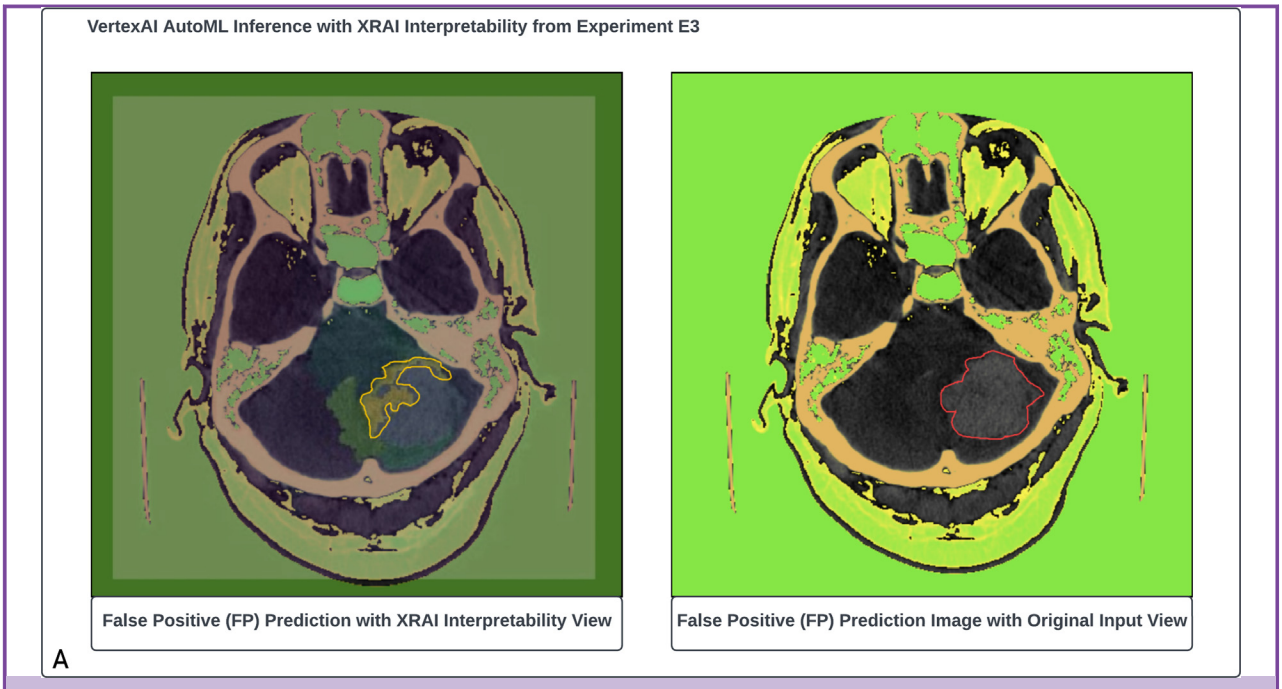

FIGURE 4. VertexAI AutoML inference results from the experiment E3. (A) One false-positive prediction inference example derived from experiment E3 with the XRAI interpretation results due to human label error. The red polygon was the annotation provided by a senior neurologist at Mayo Clinic (WDF) and indicates a true ICH-positive lesion. The yellow polygon was highlighted by the XRAI corresponding as well of this false-positive label VertexAI AutoML model. The XRAI outlined an area that is actually positive for IH. Also, this eXplanation with Ranked Area Integrals (XRAI) labeled region was reviewed by clinical neurology experts as being part of the IH or possible cerebellar brain edema. ICH, intracerebral hemorrhage; IH, intracranial hemorrhage.

patients for transportation to larger stroke centers, and similar to emerging complex big data computer vision systems.[41] The coauthor (WDF) used BARD, a conversational generative AI chatbot developed by Google, to generate the acronym HEADS-UP to signify its purpose as an acronym. Hence, HEADS-UP helps draw attention to the currently limited care in underserved areas around the globe for IH detection, a debilitating disease that requires timely intervention and efficient management (Figure 3).

Out of the 4 experiments conducted through our AutoML model, experiment E4 was conducted on 6000 combined RGB images and achieved the highest values regarding average precision (95.80%), optimal precision (91.40%), and recall (91.40%). This emphasizes the importance of levitating the capability of AutoML in detecting IH positive cases from NCCT images. In addition, experiment E4 outperformed the remaining 3 experiments with a 4.30%, 0.60%, and 0.60% boost respectively, in average precision. This suggests that increasing the training sample size with appropriate image preprocessing could boost the performance of binary IH classification.

However, given the ability of XRAI to interpret AutoML predictions, we believe that the annotations provided by the RSNA dataset were not entirely accurate. For instance, in Figure 4, one of the testing results using XRAI in E3 considered the available image extracted from the RSNA dataset as ICH negative. At the same time, our AutoML model predicted it as ICH-positive and labeled it with a yellow polygon. This was consistent with a subsequent evaluation by a senior neurosurgeon in our department, who used the red polygon shown in Figure 1 to highlight the same lesion. Furthermore, this red polygon contained the yellow polygon that was already highlighted by the XRAI and was confirmed as

a true positive ICH lesion. We believe this false-positive prediction is because of the incorrect labeling in the RSNA dataset.

The incorrect labels from the RSNA dataset could be the reason why our AutoML model is not achieving higher performance metrics. Hence, training an AutoML model with more accurate labels may boost performance. Furthermore, a thorough evaluation is highly recommended for the models pretrained on the RSNA dataset before clinical implementation.

To our knowledge, this is the first binary IH classifier that used XRAI for model interpretation. XRAI in Google VertexAI AutoML is considered a low-code software development approach, ensuring better team communication despite different backgrounds. Hence, we were able to rapidly develop HEADS-UP in about 2 weeks using an open dataset and assembling a team of physicians and scientists with Google Cloud and the Vertex platform. Overall, this model shows the promise of creating a deployable ML algorithm in health care in a fairly short amount of time using the formula of a domain expert (physician), scientists, computer scientists, a dataset, a clear objective, and a scalable platform.

Wang et al[42] reported a similar binary IH classifier that used class activation mapping to find the regions contributing to predicting the classification model. They directly used 674,258 2-dimensional scans for model development and generated a 95.8% recall from a completely different test set than ours.[42] In comparison, we started applying our model to a small sample size and expanded in size to understand the correlation between sample size and performance more thoroughly. Furthermore, as described previously, we applied XRAI interpretation and manual qualitative evaluation by an expert neurosurgeon. Hence, we concluded that the labels provided in the original RSNA hemorrhage dataset lack complete accuracy. We believe such mislabeling could cause a considerable risk of misleading model predictions, especially when directly deploying models trained on the RSNA dataset clinically without a thorough clinical evaluation. Furthermore, we performed 4 experiments (Figure 1) that elevated performance metrics with a more complicated image preprocessing, whereas Wang et al[42] carried an image preprocessing similar to our E2 and E3 experiments.

Through HEADS-UP, we aim to establish intellectual independence from third-party vendors and leverage our own internal expertise and talents in developing new technologies to help future patients. We believe some models, like HEADS-UP, created using public datasets should be made open-source and given back to the public to benefit underserved populations.

CONCLUSION

Hemorrhage evaluation and detector system for underserved populations, HEADS-UP, is a rapid, cloud-based, and deployable ML method to detect IH. We are considering implementing this system across the Mayo Clinic enterprise and expanding to include underserved areas to help patients and their clinical teams. Using Google VertexAI and AutoML helps teams iterate rapidly to create fairly high accuracy models very quickly and prevents a team from having to write custom code models, which can take much longer.

POTENTIAL COMPETING INTERESTS

All authors declare that they have no conflict of interest.

SUPPLEMENTAL ONLINE MATERIAL

Supplemental material can be found online at https://www.mcpdigitalhealth.org/. Supplemental material attached to journal articles has not been edited, and the authors take responsibility for the accuracy of all data.

Abbreviations and Acronyms: **HEADS-UP,** hemorrhage evaluation and detector system for underserved populations; **IH,** intracranial hemorrhage; **ICH,** intracerebral hemorrhage; **ML,** machine learning; **NCCT,** noncontrast head CT scans; **RGB images,** R(red), G(green), and B(blue) images; **RSNA,** radiological society of North America

Correspondence: Address to W. David Freeman, MD, 4500 San Pablo Road, Jacksonville, FL 32224 (freeman.william1@mayo.edu).

ORCID

Saif Salman: https://orcid.org/0000-0002-7809-1745William David Freeman: https://orcid.org/0000-0003-2326-0633

REFERENCES

1. Katan M, Luft A. Global burden of stroke. *Semin Neurol*. 2018; 38(2):208-211. https://doi.org/10.1055/s-0038-1649503.
2. O'Carroll CB, Brown BL, Freeman WD. Intracerebral hemorrhage: A common yet disproportionately deadly stroke subtype. *Mayo Clin Proc*. 2021;96(6):1639-1654. https://doi.org/10.1016/j.mayocp.2020.10.034.
3. Naidech AM. Intracranial hemorrhage. *Am J Respir Crit Care Med*. 2011;184(9):998-1006. https://doi.org/10.1164/rccm.201103-0475CI.
4. Greenberg SM, Ziai WC, Cordonnier C, et al. 2022 Guideline for the management of patients with spontaneous intracerebral hemorrhage: a guideline from the American Heart Association/American Stroke Association. *Stroke*. 2022;53(7):e282-e361. https://doi.org/10.1161/STR.0000000000000407.
5. Flaherty ML, Woo D, Haverbusch M, et al. Racial variations in location and risk of intracerebral hemorrhage. *Stroke*. 2005; 36(5):934-937. https://doi.org/10.1161/01.STR.0000160756.72109.95.
6. Ziai WC, Carhuapoma JR. Intracerebral hemorrhage. *Continuum (Minneap Minn)*. 2018;24(6):1603-1622. https://doi.org/10.1212/CON.0000000000000672.
7. van Asch CJ, Luitse MJ, Rinkel GJ, van der Tweel I, Algra A, Klijn CJ. Incidence, case fatality, and functional outcome of intracerebral haemorrhage over time, according to age, sex, and ethnic origin: a systematic review and meta-analysis. *Lancet Neurol*. 2010;9(2):167-176. https://doi.org/10.1016/S1474-4422(09)70340-0.
8. Hart RG, Tonarelli SB, Pearce LA. Avoiding central nervous system bleeding during antithrombotic therapy: recent data and ideas. *Stroke*. 2005;36(7):1588-1593. https://doi.org/10.1161/01.STR.0000170642.39876.f2.
9. Summers D, Leonard A, Wentworth D, et al. Comprehensive overview of nursing and interdisciplinary care of the acute ischemic stroke patient: a scientific statement from the American Heart Association. *Stroke*. 2010 Sep;41(9):e563. Published correction appears in *Stroke*. 2011;42(3):e357. https://doi.org/10.1161/STROKEAHA.109.192362
10. Blacquiere D, Demchuk AM, Al-Hazzaa M, et al. Intracerebral hematoma morphologic appearance on noncontrast computed tomography predicts significant hematoma expansion. *Stroke*. 2015;46(11):3111-3116. https://doi.org/10.1161/STROKEAHA.115.010566.
11. Gong K, Dai Q, Wang J, et al. Unified ICH quantification and prognosis prediction in NCCT images using a multi-task interpretable network. *Front Neurosci*. 2023;17:1118340. https://doi.org/10.3389/fnins.2023.1118340.
12. Cai J, Zhu H, Yang D, et al. Accuracy of imaging markers on noncontrast computed tomography in predicting intracerebral hemorrhage expansion. *Neurol Res*. 2020;42(11):973-979. https://doi.org/10.1080/01616412.2020.1795577.
13. Hillal A, Sultani G, Ramgren B, Norrving B, Wassélius J, Ullberg T. Accuracy of automated intracerebral hemorrhage volume measurement on non-contrast computed tomography: a Swedish Stroke Register cohort study. *Neuroradiology*. 2023; 65(3):479-488. https://doi.org/10.1007/s00234-022-03075-9.
14. Jain A, Malhotra A, Payabvash S. Imaging of spontaneous intracerebral hemorrhage. *Neuroimaging Clin N Am*. 2021;31(2):193-203. https://doi.org/10.1016/j.nic.2021.02.003.
15. Marcolini E, Hine J. Approach to the diagnosis and management of subarachnoid hemorrhage. *West J Emerg Med*. 2019;20(2): 203-211. https://doi.org/10.5811/westjem.2019.1.37352.
16. Romanova AL, Nemeth AJ, Berman MD, et al. Magnetic resonance imaging versus computed tomography for identification and quantification of intraventricular hemorrhage. *J Stroke Cerebrovasc Dis*. 2014;23(8):2036-2040. https://doi.org/10.1016/j.jstrokecerebrovasdis.2014.03.005.
17. Brott T, Broderick J, Kothari R, et al. Early hemorrhage growth in patients with intracerebral hemorrhage. *Stroke*. 1997;28(1):1-5. https://doi.org/10.1161/01.str.28.1.1.
18. Code ICH. Code ICH. https://code-ich.org/. Accessed August 14, 2023.
19. Ramos LA, van der Steen WE, Sales Barros R, et al. Machine learning improves prediction of delayed cerebral ischemia in patients with subarachnoid hemorrhage. *J Neurointerv Surg*. 2019; 11(5):497-502. https://doi.org/10.1136/neurintsurg-2018-014258.
20. de Jong G, Aquarius R, Sanaan B, et al. Prediction models in aneurysmal subarachnoid hemorrhage: forecasting clinical outcome with artificial intelligence. *Neurosurgery*. 2021;88(5): E427-E434. https://doi.org/10.1093/neuros/nyaa581.
21. Silva MA, Patel J, Kavouridis V, et al. Machine learning models can detect aneurysm rupture and identify clinical features associated with rupture. *World Neurosurg*. 2019;131:e46-e51. https://doi.org/10.1016/j.wneu.2019.06.231.
22. Vagal A, Saba L. Artificial intelligence in "code stroke"-A paradigm shift: do radiologists need to change their practice? *Radiol Artif Intell*. 2022;4(2):e210204. https://doi.org/10.1148/ryai.210204.
23. Mouridsen K, Thurner P, Zaharchuk G. Artificial intelligence applications in stroke. *Stroke*. 2020;51(8):2573-2579. https://doi.org/10.1161/STROKEAHA.119.027479.
24. Nishi H, Oishi N, Ishii A, et al. Predicting clinical outcomes of large vessel occlusion before mechanical thrombectomy using machine learning. *Stroke*. 2019;50(9):2379-2388. https://doi.org/10.1161/STROKEAHA.119.025411.
25. Chen Z, Zhang R, Xu F, et al. Novel prehospital prediction model of large vessel occlusion using artificial neural network. *Front Aging Neurosci*. 2018;10:222. https://doi.org/10.3389/fnagi.2018.00222.
26. Hassan AE, Ringheanu VM, Preston L, Tekle WG. Artificial intelligence—parallel stroke workflow tool improves reperfusion rates and Door-In to puncture interval. *Stroke Vasc Interv Neurol*. 2022;2(5):e000224. https://doi.org/10.1161/SVIN.121.000224.
27. Bruggeman AAE, Koopman MS, Soomro J, et al. Automated detection and location specification of large vessel occlusion on computed tomography angiography in acute ischemic stroke. *Stroke Vasc Interv Neurol*. 2022;2(4):e000158. https://doi.org/10.1161/SVIN.121.000158.
28. Flanders AE, Prevedello LM, Shih G, et al. Construction of a machine learning dataset through collaboration: the RSNA 2019 brain CT hemorrhage challenge. Published correction appears in *Radiol Artif Intell*. 2020;2(4):e209002. *Radiol Artif Intell*. 2020;2(3):e190211. https://doi.org/10.1148/ryai.2020209002.
29. Bidgood WD Jr, Horii SC, Prior FW, Van Syckle DE. Understanding and using DICOM, the data interchange standard for biomedical imaging. *J Am Med Inform Assoc*. 1997;4(3):199-212. https://doi.org/10.1136/jamia.1997.0040199.
30. DenOtter TD, Schubert J. Hounsfield Unit. In: *StatPearls*. StatPearls Publishing; 2023.
31. Pulmonary embolism detection. RSNA. https://www.rsna.org/education/ai-resources-and-training/ai-image-challenge/RSNA-pe-detection-challenge-2020. Accessed August 14, 2023.
32. Kapishnikov A, Bolukbasi T, Viegas F, Terry M. XRAI: better attributions through regions. In: International CVF, ed. *Conference on Computer Vision (ICCV)*. vol 2019. IEEE Publications; 2019: 4947-4956. https://doi.org/10.1109/ICCV.2019.00505.
33. Lemesle M, Giroud M, Menassa M, Milan C, Dumas R. Incidence and case-fatality rates of stroke in Burgundy (France). Comparison between a rural (Avallon) and an urban (Dijon) population, between 1989 and 1993. *Eur J Neurol*. 1996;3(2): 109-115. https://doi.org/10.1111/j.1468-1331.1996.tb00201.x.
34. Garbusinski JM, van der Sande MA, Bartholome EJ, et al. Stroke presentation and outcome in developing countries: a

prospective study in the Gambia. *Stroke*. 2005;36(7):1388-1393. https://doi.org/10.1161/01.STR.0000170717.91591.7d.

35. Okon NJ, Rodriguez DV, Dietrich DW, et al. Availability of diagnostic and treatment services for acute stroke in frontier counties in Montana and Northern Wyoming. *J Rural Health*. 2006;22(3):237-241. https://doi.org/10.1111/j.1748-0361.2006.00038.x.
36. Liu M, Wu B, Wang WZ, Lee L, Zhang S, Kong L. Stroke in China: epidemiology, prevention, and management strategies. *Lancet Neurol*. 2007;6(5):456-464. https://doi.org/10.1016/S1474-4422(07)70004-2.
37. Brainin M, Teuschl Y, Kalra L. Acute treatment and long-term management of stroke in developing countries. *Lancet Neurol*. 2007;6(6):553-561. https://doi.org/10.1016/S1474-4422(07)70005-4.
38. Davis MA, Rao B, Cedeno PA, Saha A, Zohrabian VM. Machine learning and improved quality metrics in acute intracranial hemorrhage by noncontrast computed tomography. *Curr Probl Diagn Radiol*. 2022;51(4):556-561. https://doi.org/10.1067/j.cpradiol.2020.10.007.
39. Arbabshirani MR, Fornwalt BK, Mongelluzzo GJ, et al. Advanced machine learning in action: identification of intracranial hemorrhage on computed tomography scans of the head with clinical workflow integration. *npj Digit Med*. 2018;1:9. https://doi.org/10.1038/s41746-017-0015-z.
40. Lyu J, Xu Z, Sun H, Zhai F, Qu X. Machine learning-based CT radiomics model to discriminate the primary and secondary intracranial hemorrhage. *Sci Rep*. 2023;13(1):3709. https://doi.org/10.1038/s41598-023-30678-w.
41. Zhou B, Khosla A, Lapedriza A, Torralba A, Oliva A. Places: an image database for deep scene understanding. Preprint. Posted online October 6, 2016. arxiv.org/abs/1610.02055. doi: org/10.48550/arXiv.1610.02055
42. Wang X, Shen T, Yang S, et al. A deep learning algorithm for automatic detection and classification of acute intracranial hemorrhages in head CT scans. *NeuroImage Clin*. 2021;32:102785. https://doi.org/10.1016/j.nicl.2021.102785.